JOURNAL OF AIRCRAFT
Vol. 38, No. 1, January–February 2001

Structural Wing Sizing for Multidisciplinary Design Optimization of a Strut-Braced Wing

Frank H. Gern,* Amir H. Naghshineh-Pour,† Erwin Sulaeman,‡ and Rakesh K. Kapania§
Virginia Polytechnic Institute and State University, Blacksburg, Virginia 24061-0203
and
Raphael T. Haftka¶
University of Florida, Gainesville, Florida 32611-6250

A structural and aeroelastic model for wing sizing and weight calculation of a strut-braced wing is described. The wing weight is calculated using a newly developed analysis accounting for the special nature of strut-braced wings. A specially developed aeroelastic model enables one to consider wing flexibility and spanwise redistribution of the aerodynamic loads during in-flight maneuvers. The structural model uses a hexagonal wing-box featuring skin panels, stringers, and spar caps, whereas the aerodynamics part employs a linearized transonic vortex lattice method. Thus, the wing weight may be calculated from the rigid or flexible wing spanload. The calculations reveal the significant influence of the strut on the bending material weight of the wing. The strut enables one to design a wing featuring thin airfoils without weight penalty. It also influences the spanwise redistribution of the aerodynamic loads and the resulting deformations. Increased weight savings are possible by iterative resizing of the wing structure using the actual design loads. As an advantage over the cantilever wing, the twist moment caused by the strut force results in increased load alleviation, leading to further structural weight savings.

Nomenclature

AR	=	wing aspect ratio
b	=	wing span
c	=	wing chord
c_b	=	wing-box chord
d	=	airfoil thickness
F_{sh}	=	horizontal strut force, y direction
F_{sv}	=	vertical strut force, z direction
$I(y)$	=	wing-box cross-sectional moment of inertia
L_{off}	=	strut vertical offset length
$M(y)$	=	bending moment
M_∞	=	freestream Mach number
$q_i(y)$	=	lift force per unit length for element i
s	=	wing/strut intersection (from wing root)
t	=	wing skin thickness
u	=	unit step function
u_{ab}, v_{ab}, w_{ab}	=	backwash, sidewash, and downwash velocity, respectively
$V(y)$	=	shear force
W_e	=	engine weight
w	=	bending deflection
y	=	spanwise coordinate
y_e	=	spanwise engine position (from root)
α, β	=	lift coefficients at structural nodes
Γ	=	vortex strength
θ	=	bending slope
Λ	=	wing sweep angle
σ_{all}	=	allowable stress
$\sigma_{\max}$	=	maximum stress

Received 6 October 1999; revision received 5 June 2000; accepted for publication 7 July 2000.

*Research Associate, Department of Aerospace and Ocean Engineering; currently Research Assistant Professor, Center for Intelligent Material Systems and Structures, Blacksburg, VA 24061-0261. Member AIAA.

†Graduate Student, Department of Aerospace and Ocean Engineering; currently Aerospace Structures Engineer, B.F. Goodrich Aerospace, Aerostructures Group, Chula Vista, CA 91910-2098. Student Member AIAA.

‡Graduate Student, Department of Aerospace and Ocean Engineering.

§Professor, Department of Aerospace and Ocean Engineering. Associate Fellow AIAA.

¶Distinguished Professor, Department of Aerospace Engineering, Mechanical and Engineering Sciences. Fellow AIAA.

Introduction

STRUT-BRACED wing configurations have been used both in the early days of aviation and today's small airplanes. Adopting thin airfoil sections required external structural wing support to sustain the aerodynamic loads. However, external structures cause a significant drag penalty. Gradually, it was understood that the external bracing could be removed, and lower drag could be achieved by replacing the wing-bracing structure with a cantilever wing with an appropriate wing-box and thickness to chord ratios.

However, along with the idea of the cantilever wing configuration with its aerodynamic advantages, the concept of the truss-braced wing configuration also survived. This is due to the tireless efforts of Pfenninger at Northrop in the early 1950s[1] and his continuation of these efforts until the late 1980s. Using a strut or a truss offers the opportunity to increase the wing aspect ratio and to decrease the induced drag significantly without wing weight penalties relative to a cantilever wing. Also, a lower wing thickness becomes feasible reducing transonic wave drag and, hence, resulting in a lower wing sweep. Reduced wing sweep and high aspect ratios produce natural laminar flow due to low Reynolds numbers. Consequently, a significant increase in the overall aircraft performance is achieved.[2,3]

A number of strut-braced wing aircraft configurations have been investigated in the past. Kulfan and Vachal from The Boeing Company performed preliminary design studies and evaluated the performance of a large subsonic military airplane.[4] They compared performance and economics of a cantilever wing with a strut-braced wing configuration. Two load conditions, a 2.5-g maneuver and 1.67-g taxi bump were used to perform structural analyses. Their optimization and sensitivity analyses showed that high aspect ratio wings with low thickness to chord ratios would result in a significant fuel consumption reduction.

For the cantilever configuration, a ground strike problem arose during taxiing. This issue was resolved by adding a strut to the wing structure. Moreover, the analysis indicated that the strut-braced wing configuration requires less fuel (1.6%) and results in lower takeoff

gross weight (1.8%) and lower empty weight (3%) compared to the cantilever wing configuration. Cost comparisons showed that, because of a lower takeoff gross weight, the operating costs of the strut-braced wing configuration were slightly less than those of the cantilever wing configuration.

Park from The Boeing Company compared the block fuel consumption of a strutted wing vs a cantilever wing.[5] He concluded that the use of a strut saves structural wing weight. However, the significant increase in the strut t/c to cope with strut buckling at the -1.0-g load condition increased the strut drag. Therefore, because of a higher fuel consumption compared to the cantilever case, the strut did not appear practical for this transport aircraft.

Another study on strut-braced wing configurations was conducted by Turriziani et al.[6] They addressed fuel efficiency advantages of a strut-braced wing business jet of aspect ratio 25 over an equivalent conventional wing business jet with the same payload and range. For the strut-braced wing design, the combined wing/strut weight was higher than for the cantilever wing. However, the strut-braced wing configuration reduced the total aircraft weight due to the aerodynamic advantages of high aspect ratio wings. Further studies showed fuel weight savings of 20%.

The strut-braced wing concept offers the possibility to reduce wing thickness without the penalty of an increased structural weight by reducing the bending moment acting on the wing. However, a reduced wing thickness together with shorter wing chords result in smaller wing-box dimensions, thus significantly reducing wing-box torsional stiffness and rendering the wing more sensitive to aeroelastic problems such as increased static aeroelastic deformation or reduced flutter and divergence speeds. The present approach highlights a possibility to remedy the problem of increased aeroelastic deformations by employment of the moment induced on the wing by a strut.

Previously investigated strut-braced wing concepts considered the strut to be rigidly attached to the wing. Therefore, strut buckling during negative load factors was a major design issue, rendering the strut very heavy to overcome this buckling constraint.[4,5] To avoid strut buckling, the present approach offers an innovative concept. A telescoping sleeve mechanism is employed to have the strut active only during positive load factors. For negative load factors, the wing acts like a cantilever wing, rendering the strut buckling constraint unnecessary. Furthermore, this arrangement allows one to apply a defined strut force at the 2.5-g maneuver design load instead of the statically indeterminate one obtained from a rigid strut attachment. This way, the strut force as well as strut position can be optimized to achieve the maximum benefits out of the design concept.

To fully exploit the synergism from the strut-braced wing concept, a multidisciplinary design optimization (MDO) approach has been chosen for aircraft design optimization. The multidisciplinary optimization problem considers aerodynamics, structures, and a detailed investigation of interference drag. The aerodynamic analysis uses simple models for induced drag, parasite drag, and interference drag. All analyses are linked together, and the performance of the strut-braced wing aircraft is then optimized for minimum takeoff gross weight.[3,7,8]

The MDO approach has been implemented in several aircraft designs. Grossman et al.[9] investigated the interaction of aerodynamic and structural design of a composite sailplane subject to aeroelastic, structural, and aerodynamic constraints to increase the overall performance. They showed that MDO can yield results superior to the ones obtained from the sequential method. Another example is the application of MDO to a high-speed civil transport (HSCT). A significant effort has been made at the Multidisciplinary Analysis and Design center of Virginia Polytechnic Institute and State University to perform MDO of an HSCT. Several methods were developed for better use of the MDO approach for aircraft conceptual and preliminary design. More information about this work can be obtained from Refs. 10 and 11.

The presented wing sizing module provides two essential features within the MDO environment. First, it is used to calculate the structural wing weight, that is, the bending material weight of the wing-box. It has been found that commonly available wing weight calculation routines such as the NASA Langley Research Center developed Flight Optimization System (FLOPS)[12] are not accurate enough for the present approach. Therefore, a computer program was developed to accurately calculate the bending material weight of the wing based on a double plate model. The nonstructural wing weight such as that of flaps, slats, spoilers, ribs, etc., is still calculated from the FLOPS equations by replacing the FLOPS bending material weight by the actual one.

Second, the wing sizing module features an idealized hexagonal wing-box model that has been provided for the project by Lockheed Martin Aeronautical Systems in Marietta, Georgia. The hexagonal wing-box permits accurate computation of the wing's torsional stiffness, therefore enabling one to investigate aeroelastic effects, such as static aeroelastic deformation and maneuver load alleviation, and to use flexible spanload distributions as design loads. As a result, the model can be employed to resize the wing according to the actual in-flight maneuver loads. This procedure usually leads to significant wing weight reductions.

Structural Wing Modeling

Because of the unconventional nature of the proposed wing concept, commonly available weight calculation models for transport aircraft are relatively inaccurate. A special bending weight calculation procedure was thus developed, taking into account the influence of the strut on the structural wing design. In addition to the strut design, a vertical strut offset was considered to achieve a significant reduction in wing/strut interference drag.

Load Cases

To determine the bending material weight of the strut-braced wing, two maneuver load conditions (2.5-g maneuver and -1.0-g pushover) and a taxi bump (-2.0 g) are considered to be the critical design cases. For the -1.0-g pushover and for the -2.0-g taxi bump, the strut is not active and the wing acts as a cantilever beam. Because the strut is not supporting the wing in these cases, very high deflections of the wing are expected for the -2.0-g taxi bump. As a result, an optimization procedure is implemented to distribute the bending material to prevent wing ground strikes. To maximize the beneficial influence of the strut on the wing structure, strut force and spanwise position of the wing/strut intersection are optimized by the MDO code for the 2.5-g maneuver load case.

To attain acceptable aerodynamic characteristics of the strut, an airfoil cross section is considered. The strut is designed in such a way that it will not carry aerodynamic loads during cruise.

Structural Assumptions

Preliminary studies have shown buckling of the strut under the -1.0-g load condition to be the critical structural design requirement in the single-strut configuration, resulting in high strut weights.[3] To address this issue, an innovative design strategy that employs a telescoping sleeve mechanism to allow the strut to be inactive during negative gravitational acceleration maneuvers and active during positive gravitational acceleration maneuvers is used. Thus, during the -1.0-g maneuver, the wing acts as a cantilever beam, and for the positive gravitational acceleration maneuvers, the wing is a strut-braced beam.

Even more reduction in wing weight can be obtained by optimizing the strut force and wing/strut junction location. For a typical optimum single-strut design, this means that the strut would first engage in tension at some positive, a priori determined, load factor. This can be achieved by providing a slack in the wing/strut mechanism. The optimum strut force at 2.5-g is different from the strut force that would be obtained at 2.5-g if the strut were engaged for all positive values of the load factor.

The slack load factor is defined as the load factor at which the strut initially engages. It is important to have the slack load factor always positive, otherwise the strut would be preloaded at the jig shape of the wing to achieve the optimum strut force. To prevent the strut from engaging and disengaging during cruise due to gust

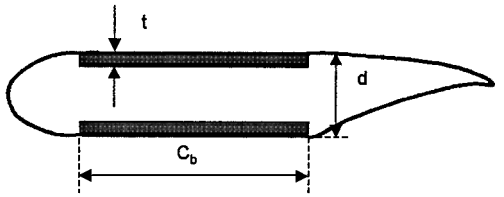

Fig. 1 Double plate model for bending weight calculation.

loads, the upper limit for the slack load factor is set to 0.8 during the optimization.

Double Plate Model

For calculation of the wing bending weight of single-strut configurations, a piecewise linear load representation is used. The wing structure is idealized as a double plate model (Fig. 1). This model is made of upper and lower skin panels, which are assumed to carry the bending moment. The double plate model offers the possibility to extract the material thickness distribution by a closed-form equation.

The simplicity of this structural wing representation makes it highly effective in terms of computational time. Comparison of the results in the "Validation" section also shows its acceptable accuracy in wing weight computation. Therefore, this model was first incorporated into the MDO environment to obtain reasonable wing weight predictions. For the sake of completeness, it is briefly discussed. The drawback of the double plate model is its inability to compute any torsional stiffness, which, as will be shown in the following sections, enables one to size the wing according to the actual maneuver loads.

The cross-sectional moment of inertia of the wing-box can be expressed as

$$I(y) = t(y)c_b(y)d^2(y)\big/2 \tag{1}$$

To obtain the bending material weight, the corresponding bending stress in the wing is calculated from

$$\sigma_{\max} = \frac{M(y)d(y)}{2I(y)} \tag{2}$$

If the wing is designed according to the fully stressed criterion, the allowable stress σ_{all} can be substituted into Eq. (2) for $\sigma_{\max}$. Substituting $I(y)$ into Eq. (2), the wing panel thickness can be specified as

$$t(y) = \frac{|M(y)|}{c_b(y)d(y)\sigma_{\text{all}}} \tag{3}$$

Wing Bending Moment Distribution

The local lift distribution can be written as

$$q_i(y) = \left[\frac{(y - y_{i+1})}{(y_i - y_{i+1})}\alpha_i + \frac{(y - y_i)}{(y_{i+1} - y_i)}\beta_i\right] \tag{4}$$

where $q_i(y)$ is the lift force per unit length for element i, α_i, and β_i are the lift coefficients at nodes i and $i+1$, and y_i and y_{i+1} are the node coordinates of node i and $i+1$ in the y direction, respectively. The piecewise representation of the aerodynamic loads in global coordinates is shown in Fig. 2.

The shear force and moment equations are obtained from the spanwise lift distribution by applying the well-known beam equations. Because for the -1.0-g load case the strut is not active, the load distribution is identical to the one obtained for a cantilever wing. Therefore, it is not displayed here. For the 2.5-g maneuver case, the strut is active, which adds an additional shear force and bending moment to the wing.

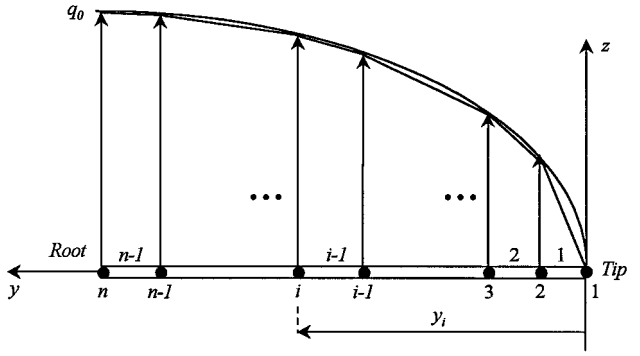

Fig. 2 Piecewise aerodynamic loads representation.

As a result, the shear force develops to

$$V(y) = W_e u\left[y - \left(\frac{b}{2} - y_e\right)\right] + F_{sv}u\left[y - \left(\frac{b}{2} - s\right)\right] - \int_0^y q(y)\,\mathrm{d}y \tag{5}$$

Consequently, the bending moment on the strut-braced wing is obtained by integration of the shear force along the span:

$$M(y) = -V(y)y - W_e e u\left[y - \left(\frac{b}{2} - y_e\right)\right] + F_{sv}\left(\frac{b}{2} - s\right) \times u\left[y - \left(\frac{b}{2} - s\right)\right] - \int_0^y yq(y)\,\mathrm{d}y + W_e\left(\frac{b}{2} - y_e\right) \times u\left[y - \left(\frac{b}{2} - y_e\right)\right] + F_{sh}L_{\text{off}}u\left[y - \left(\frac{b}{2} - s\right)\right] \tag{6}$$

In Eq. (6), $u[y]$ is the Heaviside function. The structural boundary conditions are

$$\theta(b/2) = 0 \tag{7a}$$

$$w(b/2) = 0 \tag{7b}$$

The calculated panel thickness is modified by the results obtained from the tip displacement constraint optimization. Therefore, the bending material weight of the half-wing is

$$W_{wb} = 2\int_0^{b_s/2} t(y)c_b(y)\rho\,\mathrm{d}y \tag{8}$$

where b_s is the structural span with $b_s = b/\cos\Lambda$.

Vertical Strut Offset

To reduce the wing/strut interference drag, a vertical offset between strut and wing is provided. The vertical offset member is designed for a combined bending/tension loading. In this context, the horizontal component of the strut force is of special concern (Fig. 3). Because this horizontal force results in a considerable bending load on the offset piece, its weight increases dramatically with increasing strut force and offset length.

As a result, it is imperative to employ MDO tools to obtain optimum values for vertical offset, strut force, and spanwise wing/strut breakpoint. This way, it is possible to tradeoff two contrary design requirements: 1) reduced offset length to reduce strut loading and 2) increased offset length to reduce wing/strut interference drag. After a complete design optimization with the vertical strut offset as an active design variable, the influence of the offset weight on the total strut weight becomes comparably small. For the wing bending weight and takeoff gross weight (TOGW), the weight impact of the vertical strut offset becomes almost immaterial.

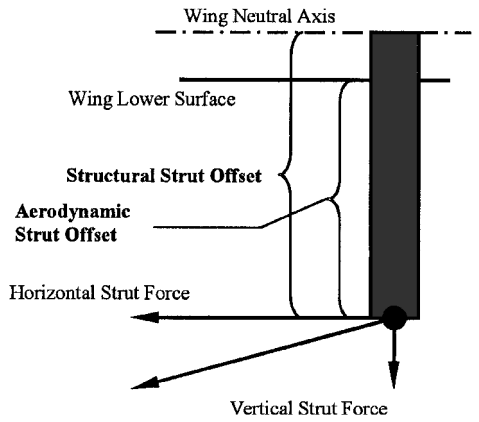

Fig. 3 Vertical strut offset and applied loads.

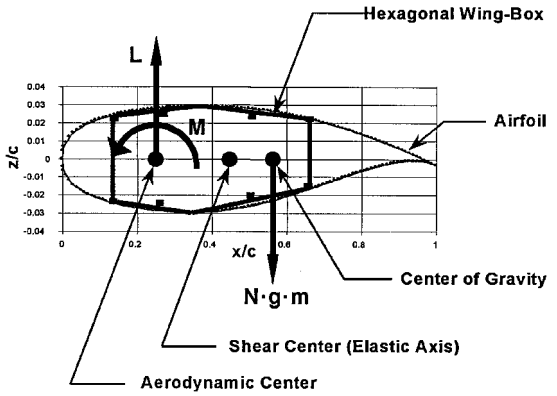

Fig. 4 Hexagonal wing-box and applied sectional forces and moments.

Hexagonal Wing-Box Model

Although the double plate model gives very accurate estimates for the wing bending material weight, it is not suitable for calculation of the wing-box torsional stiffness. This torsional stiffness becomes essential when calculating wing twist and flexible wing lift distribution (spanload), as well as for the incorporation of aeroelastic constraints into the MDO optimization.

Therefore, a hexagonal wing-box model, capable of providing torsional stiffness, was implemented into the wing weight calculation module (Fig. 4). This model was provided by Lockheed Martin Aeronautical Systems, Marietta, Georgia. Based on Lockheed Martin's experience in wing sizing, the wing-box geometry varies in the spanwise direction with optimized area and thickness ratios for spar webs, spar caps, stringers, and skins. By keeping these ratios fixed, it is still possible to reduce all geometric data of the wing-box to one independent thickness that is allowed to vary in the spanwise direction. Therefore, despite the complexity of the geometry, a closed solution for the material thickness can still be found by employing the piecewise linear load representation.

In contrast to the double plate model, the hexagonal wing-box allows computation of bending and torsional stiffness with a high degree of accuracy. Furthermore, minimum gauges and maximum stress cutoffs can be accurately applied. However, because both the double plate model and the hexagonal wing-box give very similar results for the wing bending weight, the double plate model may still be used where flexible wing sizing is not considered and computational efficiency is imperative.

Aerodynamic Modeling

The aerodynamic loads are calculated based on the well-accepted vortex lattice concept (VLM). To account for compressibility effects, the airflow density is corrected according to the upstream Mach number using a linear approximation. Although not capable of transonic shock predictions, this modification allows accurate calculations of local lift coefficients. To take into account the spanwise variation of the sectional pitch and dihedral, as well as the chordwise variation of the airfoil camber surface, the flow tangency boundary condition is formulated as

$$U_\infty \sin(\alpha - \delta)\cos\gamma = w_{ab}\cos\gamma\cos\delta + v_{ab}\sin\gamma\cos\delta - u_{ab}\cos\gamma\sin\delta \tag{9}$$

where α, γ, and δ are the angle of attack, dihedral, and slope of the mean camber line, respectively, for each point on the curved surface. The induced velocities u_{ab}, v_{ab}, and w_{ab} represent the backwash, sidewash, and downwash velocities, respectively, acting on any arbitrary point C (x_c, y_c, z_c) of the lifting surface due to a bound vortex AB having the vortex strength Γ and the endpoints A (x_a, y_a, z_a) and B (x_b, y_b, z_b) (see the Appendix).

The developed lifting surface aerodynamic code has been validated with several well-documented test cases, among them a delta wing of aspect ratio $AR = 2$, as well as the unswept and swept wings investigated by Weissinger.[13]

Flexible Wing Sizing

For accurate wing sizing, the wing has been subdivided into 81 structural nodes representing the spanwise grid points for the application of the piecewise linear loads. To account for increasing gradients in the spanload toward the wing tip, cosine spacing is being used. The aerodynamic lifting surface features 40 spanwise and 5 chordwise vortex panels distributed equally along the wing span.

As a first step, the wing deformation including sectional twist angle, dihedral (bending slope), and deflection is calculated from the initial wing spanload. Because the aircraft wing is being optimized for mimimum induced drag by the MDO code, this initial spanload usually is close to an elliptical one.

To obtain an elliptical lift distribution during cruise, the wing is being pretwisted and jig twisted. The pretwist of the wing planform is calculated using Lamar's design program LAMDES.[14] Because, for a swept wing, the sectional streamwise angle of attack is a combination of twist angle and bending slope, the wing bending deformation significantly influences the aerodynamic effectiveness of the lifting surface. Therefore, to achieve the desired twist distribution of the wing during cruise, the wing is jig twisted to account for the changes in the local twist due to the bending deformation.

Gimmestad showed that consideration of the jig twist for wing sizing of the B-52 resulted in a 10% reduction in the design loads.[15] Therefore, considering the jig twist during preliminary design may result in significant structural weight savings. This holds true even more for the present case where an MDO approach allows weight savings in one component to carry through the overall design of the aircraft configuration. In the present code, the jig twist is calculated from the actual wing deformation by subtracting the bending slope from the structural twist of the wing-box.

In the following iterative procedure, the lift distribution is recalculated according to the actual wing deformation, which yields a new (flexible) spanload. Considering the new spanload, all structural wing parameters such as bending stiffness, torsional stiffness, and wing weight are recalculated and used for computation of the flexible spanload. The wing bending weight is calculated using the panel thickness results or hexagonal wing-box cross sections from the piecewise linear load model for the different load cases. The overall panel thickness distribution of the wing is obtained by considering the highest value of the panel thickness or cross section at each spanwise position (envelope).[8] To sustain the total lift for the respective load cases, the total aircraft incidence is recalculated after each iteration step, thus ensuring the correct lift for in-flight maneuvers.

The total wing weight, that is, including the secondary structure such as ribs, flaps, etc., is calculated using the FLOPS equations.[12] For this purpose, the bending material weight in FLOPS is being replaced by the bending material weight obtained from the present model.

Validation

To check the integrity of the results, the structural analysis code has been validated using available data for the 747-100. The bending

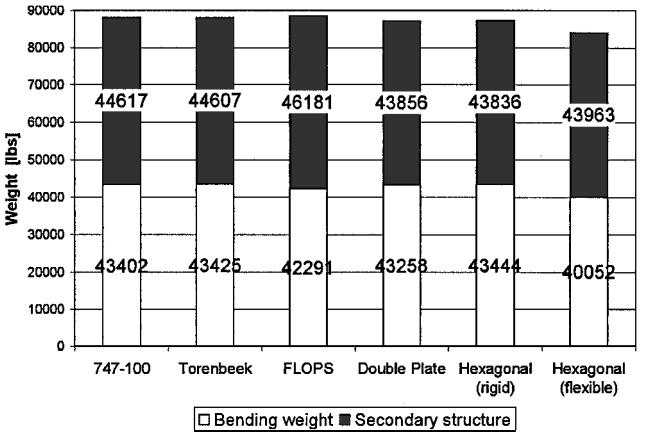

Fig. 5 Comparison of wing bending material weights and total wing weights for the 747-100 type wing.

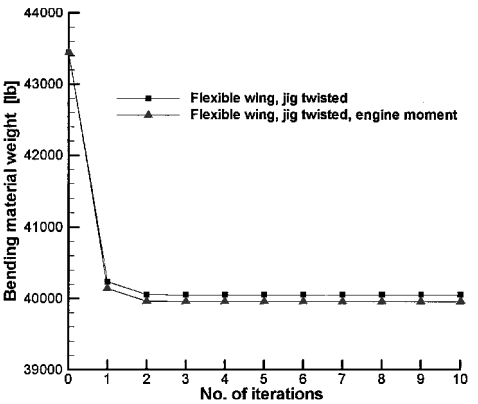

Fig. 6 Bending material weight convergence history for a 747-100-type wing.

material weight computed from the piecewise linear load model is compared with the bending material weights given by Torenbeek[16] and FLOPS.[12] Figure 5 highlights the good agreement between the weights of both the double plate and the hexagonal wing-box models with the 747-100 type wing using an elliptical spanload, that is, a rigid wing model. However, only the hexagonal model allows computation of the wing-box torsional stiffness, thus enabling one to consider the influence of pretwist, jig twist, and the load distribution for the flexible wing.

Figure 5 shows that the consideration of wing flexibility in the wing weight calculation as described can result in significant weight savings for a 747-100 type configuration. Interestingly, this potential has already been demonstrated with a flying derivative of this airplane, namely, the 747-400.

The bending weight convergence history for this configuration is shown in Fig. 6. The structural wing weight is rapidly converging to its final value, exhibiting only small variations after the first iteration step. The reason for this behavior is the relatively high torsional stiffness of this wing-box. Therefore, the main effect of considering the flexible wing load is due to the recalculation of the bending deformation after the first step and the resulting reduction in the sectional angle of attack (wash out). This high torsional stiffness is further manifested by the influence of the engine twist moments being very small.

The passive load alleviation due to the wash-out effect results in an inboard shifting of the lift loads and, therefore, reduced bending moments on the outboard sections of the wing. Although the wing structure is resized after each iteration step, the flexible wing spanload rapidly converges to its final distribution (Fig. 7). The wing deformation calculated for the 2.5-*g* maneuver of such an optimized wing structure is shown in Fig. 8.

Table 1 Strut-braced wing aircraft design variables

Property	Value
Wing halfspan	108.44 ft
Strut breakpoint	74.52 ft
Wing sweep (three-quarter chord)	25.98 deg
Strut sweep (three-quarter chord)	19.01 deg
Aerodynamic strut offset	2.74 ft
Wing root chord	32.31 ft
Wing breakpoint chord	14.76 ft
Wing tip chord	6.77 ft
Strut chord (root and tip)	6.62 ft
Wing root t/c	13.75%
Breakpoint t/c	7.23%
Wing tip t/c	6.44%
Strut t/c	8.0%
Strut force	215,387.1 lb
Engine nacelle diameter	12.54 ft
Fuselage diameter	20.33 ft
Wing flap area	1411.02 ft^2
Wing reference area	4237.30 ft^2
Aircraft zero fuel weight	335,590 lb
TOGW	504,833 lb

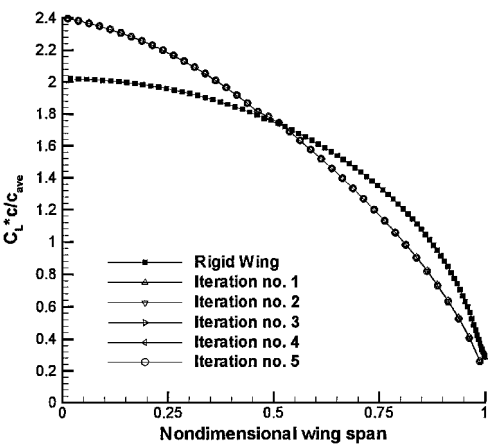

Fig. 7 Spanload convergence for the 747-100-type flexible wing.

Strut-Braced Wing Configuration

The strut-braced wing aircraft is obtained from an MDO process as described in Refs. 3 and 8 using rigid wing sizing with the structural wing weight calculated from the double plate model. For the optimization, the aircraft configuration is parameterized into 19 design variables.

Realization of a successful design requires a tight coupling of several disciplines to exploit the synergism in the strut-braced wing concept. Therefore, a multidisciplinary approach is essential. The multidisciplinary problem is broken down into aerodynamics, structures, and a detailed investigation of interference drag. The aerodynamic analysis consists of simple models for induced drag, parasite drag, and interference drag. The interference drag model is based on computational fluid dynamics analyses of various wing/strut intersection flows. A performance routine is used to evaluate the design constraints and the objective function, TOGW. All of these analyses are linked together, and the performance of the strut-braced wing is optimized with the design optimization package DOT.[17]

Using a typical long-range mission profile (cruise Mach number 0.85, range 7500 n mile, initial cruise altitude >31,000 ft, and 325 passengers) the results indicate an overall increase in performance of the strut-braced wing configuration compared to its cantilever counterpart.[8] Figure 9 and Table 1 show the details of the investigated aircraft configuration and wing design variables.

The wing design variables from Table 1 were obtained using rigid wing sizing from the double plate model. To highlight the impact of

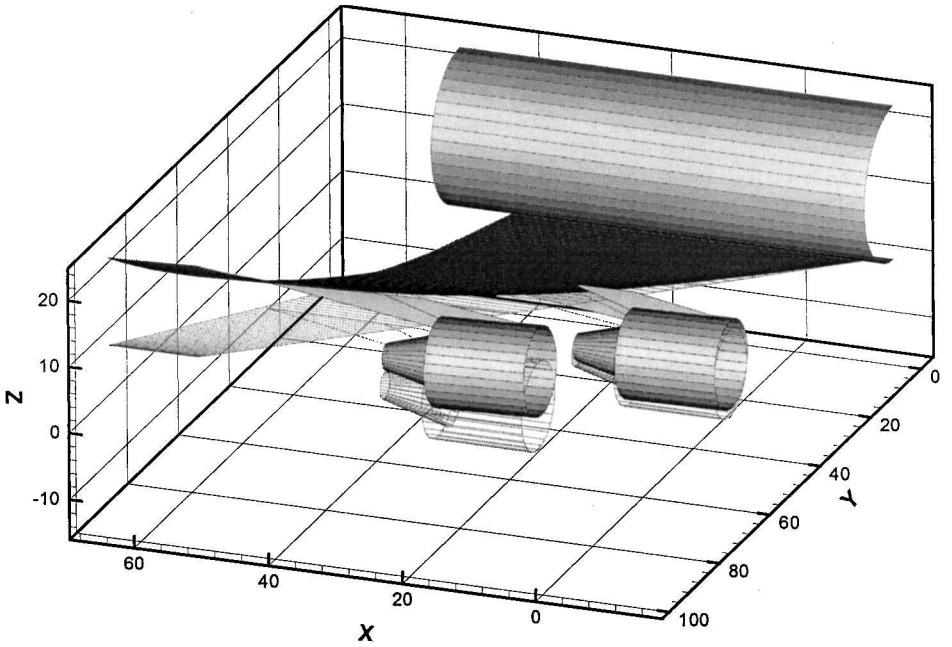

Fig. 8 Bending deformation of the 747-100-type wing configuration.

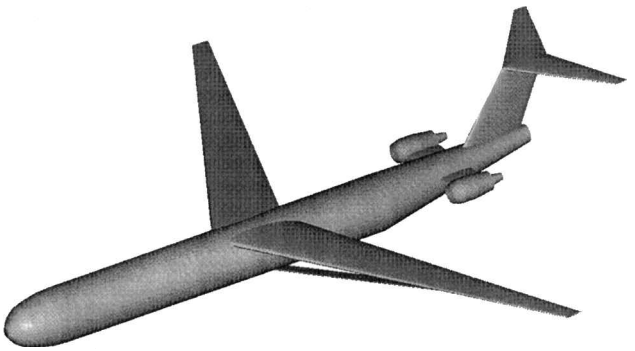

Fig. 9 Strut-braced wing with fuselage-mounted engines.

wing flexibility on the calculated wing weight, these design variables where kept constant during all subsequent analyses. The results from rigid wing sizing are being used as the baseline for comparison purposes. Because of the interdependence between wing weight and all other aircraft design variables, wing sizing from the flexible spanloads during runtime of the MDO optimization may result in a different aircraft wing configuration, making a direct comparison of rigid and flexible wing sizing more difficult.

Numerical Results

Flexible Strut-Braced Wing Spanload

The strut-braced wing as described in the preceding section has been analyzed with the new module. Figure 10 shows the spanload distribution on the wing for the 2.5-*g* maneuver obtained from the iterative process. As a first step, the wing structure was kept constant. Spanload and wing deformation were converged to their actual distributions. Basically, the strut-braced wing exhibits the same load alleviation behavior as its cantilever counterpart (Fig. 10). Because of the upward bending of the wing, lift loads are shifted inboard because of the reduction of the sectional angle of attack on the outboard wing sections (wash out). For a rigid wing, the spanload for the 2.5-*g* maneuver would be the cruise spanload scaled by the load factor 2.5, that is, an almost elliptical one.

Figure 10 also shows one major advantage of the strut-braced wing from the aeroelastic point of view: A chordwise offset of the strut attachment to the wing-box produces a twist moment acting on the wing. When the strut is attached to the wing-box front spar

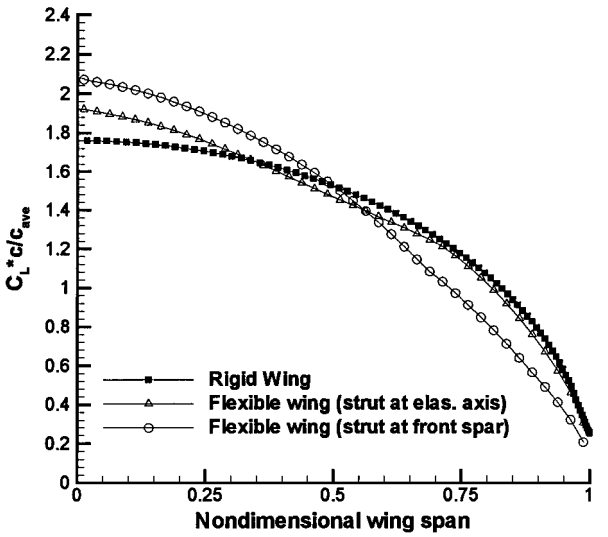

Fig. 10 Spanload distribution for the strut-braced wing in a 2.5-*g* maneuver.

instead of the wing elastic axis, this moment literally is twisting down the wing leading edge. As a result, even more load is shifted inboard, producing a much higher load alleviation effect than for a conventional wing.

As mentioned before, the aircraft incidence has to be adjusted after each iteration step to sustain the total lift for the respective load factor. As an indicator for the aircraft incidence, Figure 11 shows the convergence history of the root lift coefficient. The procedure rapidly converges toward the final value, exhibiting a behavior similar to the one observed earlier for the cantilever wing aircraft.

Wing Sizing From Flexible Spanload

Consideration of the actual maneuver spanloads usually results in a significant reduction in the design loads.[15] Because the influence of the strut moment offers even more potential for maneuver load alleviation, the impact of flexible wing sizing may even be higher than for the cantilever wing. As a next step, the wing structure has been resized according to the actual spanload distribution after each iteration step. Figure 12 shows the spanload distributions for the first five iteration steps, and Fig. 13 shows the convergence history

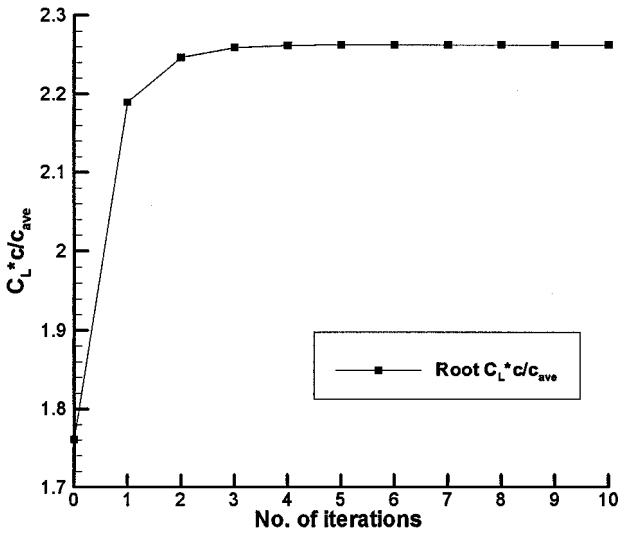

Fig. 11 Convergence history of the strut-braced wing root lift coefficient.

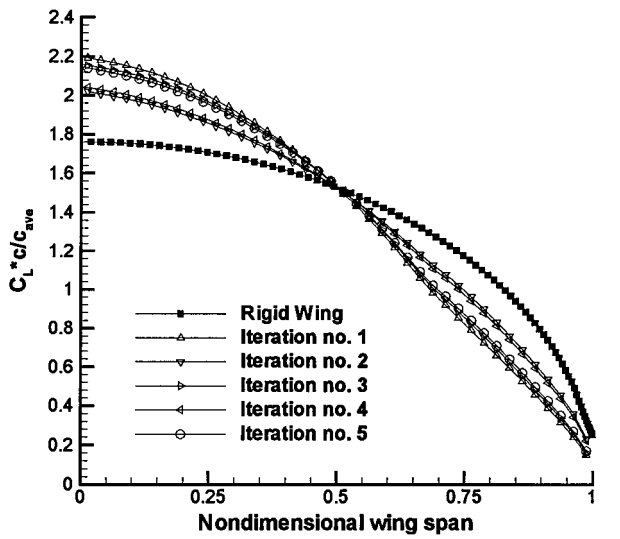

Fig. 12 Strut-braced wing spanload convergence for the 2.5-*g* maneuver; strut attached to the wing-box front spar.

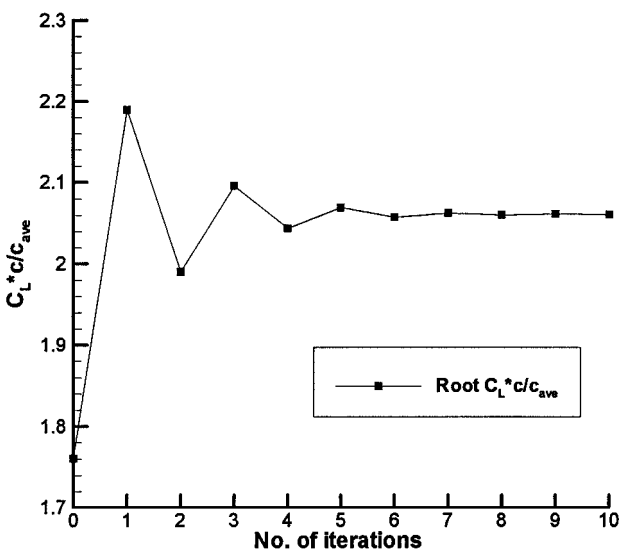

Fig. 13 Root lift coefficient convergence for the strut-braced wing in a 2.5-*g* maneuver; strut attached to wing-box front spar.

of the root lift coefficient. Because of the structural resizing, the convergence of spanload and aircraft incidence becomes slower.

Weight calculation from the design loads obtained for a flexible wing reveals the significant influence of the strut moment on maneuver load alleviation and wing weight. Figure 14 shows the convergence history of the wing bending material weight for three different strut attachments: at the wing-box front spar, in the wing elastic axis, and at the wing-box rear spar. Compared to the rigid

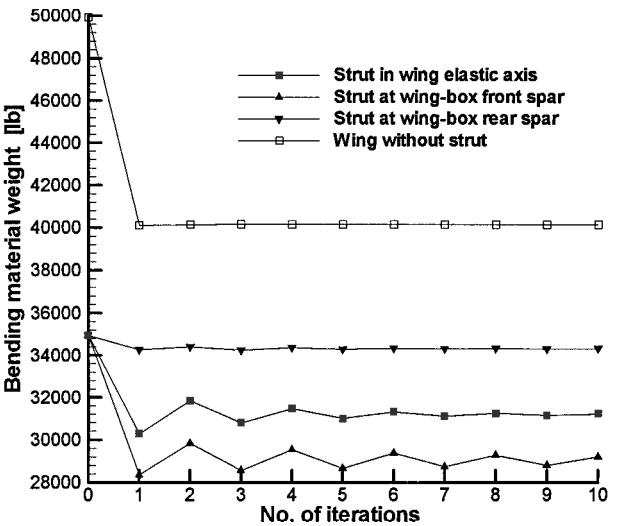

Fig. 14 Bending material weight convergence for different strut attachments.

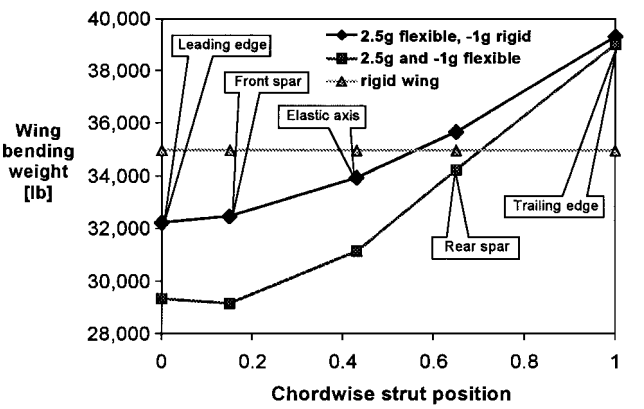

Fig. 15 Influence of the chordwise strut position on the wing bending material weight.

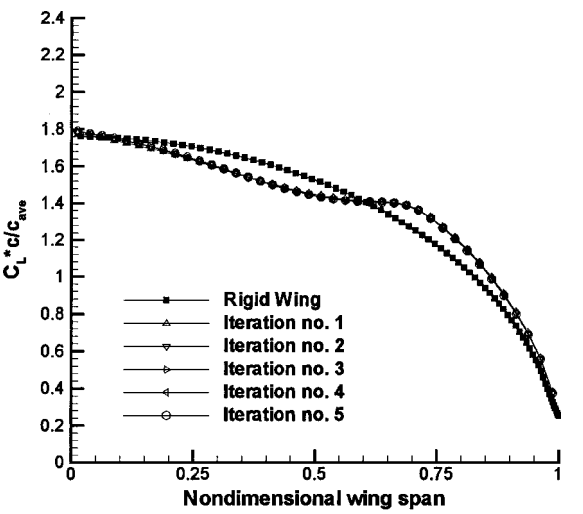

Fig. 16 Spanload convergence for the 2.5-*g* maneuver; strut attached to the wing-box rear spar.

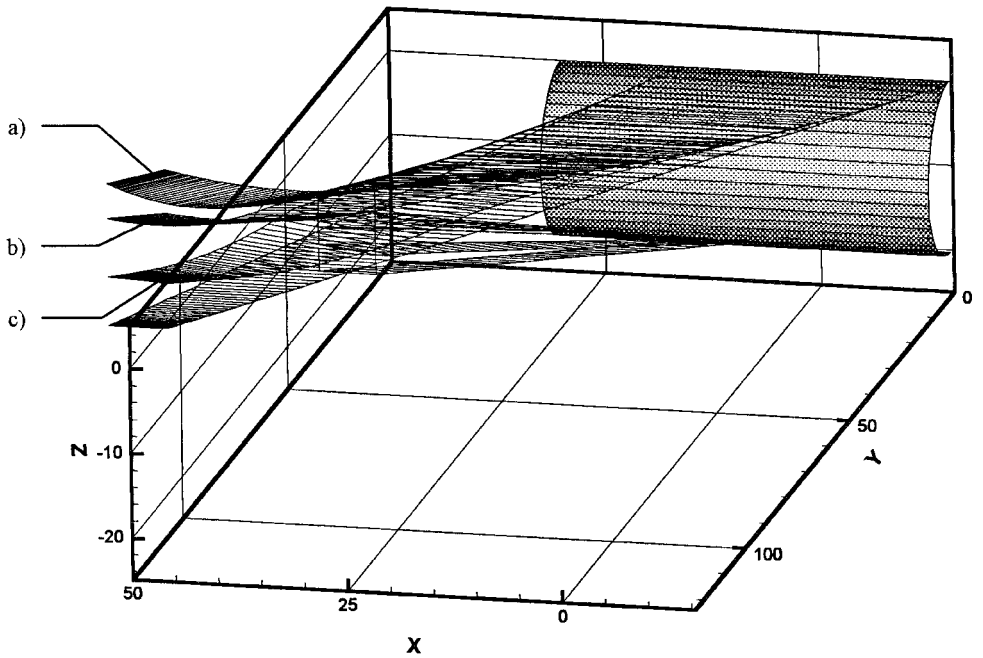

Fig. 17 Strut-braced wing deformation for the 2.5-*g* maneuver for three different chordwise strut attachment (deflections are significantly reduced when the strut is moved to the wing-box front spar): a) strut at the wing-box rear spar, b) strut at the elastic axis, and c) strut at the wing-box front spar.

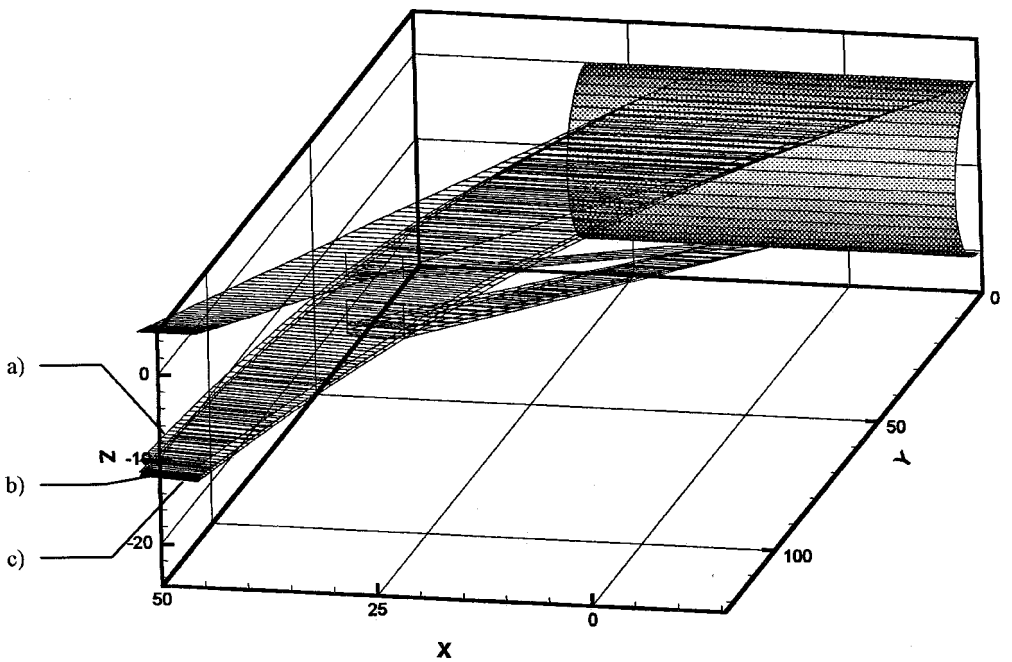

Fig. 18 Strut-braced wing downward deflections for the − 1.0-*g* pushover for three different chordwise strut attachment: a) strut at the wing-box rear spar, b) strut at the elastic axis, and c) strut at the wing-box front spar.

wing weight, sizing the wing using the actual design loads leads to lower weights for all three cases. Nevertheless, it becomes obvious that employment of the strut moment is an important design factor.

Note that an identical wing featuring a thin airfoil would suffer from significant weight penalties if designed without a strut. Figure 14 indicates a 43% weight penalty for the rigid wing sizing and a 29% weight penalty for the flexible design loads in such a case.

Figure 15 highlights the influence of the chordwise strut position on the wing bending material weight. The bending material weight increases if the strut is attached to the rear parts of the wing-box. By moving the strut backward in the chordwise direction, the influence of the strut moment is inverted, that is, it literally is pulling the leading edge upward. As a result, lift loads are shifted outboard instead of inboard. This special way of load aggravation leads to higher bending moments and higher bending material weights (Fig. 16).

The chordwise strut position and the resulting twist moment not only influence spanload and structural wing weight, but also wing bending and twist deformations. For the 2.5-*g* maneuver, the upward bending of the wing significantly decreases by moving the strut toward the leading edge of the wing (Fig. 17). In the same way, the wing twist is being reduced.

Because the strut is not active during the −1.0-*g* pushover, the downward deflections for this maneuver are relatively high. Figure 18 shows that also for the − 1.0-*g* pushover, wing deflections slightly depend on the chordwise strut position. The reason for this

behavior is that all three wings are being sized according to the actual design loads for all load cases, that is, 2.5-g maneuver, -1-g pushover, and -2-g taxi bump, with the 2.5-g maneuver load being the predominant design load. Therefore, different stiffness distributions are being obtained for all three chordwise strut attachments, leading to slightly different downward deflections even though the strut is not active.

Conclusions

A structural model for wing sizing and weight calculation of a strut-braced wing has been developed. To consider the influence of the actual design loads on the flexible wing, static aeroelastic deformations and flexible wing lift distributions have been calculated. Validation of the module with an existing aircraft wing and comparison with results from other sources showed very good agreement with the present model.

The calculations revealed the significant influence of the strut on the wing bending material weight. The use of a strut enables one to design a wing with thin airfoils without weight penalty. Designing an identical thin airfoil wing without strut would result in a 40% wing weight increase.

The strut also influences spanload distributions and wing deformations. Weight savings are possible by calculation and iterative resizing of the wing structure according to the actual design loads. Moreover, as an advantage over the cantilever wing, employment of the strut twist moment for further load alleviation leads to increased savings in structural weight.

Ongoing investigations focus on the influence of the strut on the flutter behavior of the strut-braced wing and on a complete incorporation of the flexible wing sizing routine into the strut-braced wing aircraft design process, that is, the MDO environment.

Appendix: Vortex Lattice Formulation

To calculate the aerodynamic loads on the strut-braced wing, the Biot-Sauart Law was used to derive the vortex line downwash. With $\beta = \sqrt{(1 - M_\infty^2)}$, it can be shown that the induced velocities develop into the following equations.

Downwash:

$$w_{ab}\left(\frac{\Gamma}{4\pi}\right)^{-1} =$$

$$\frac{x_{ac}y_{ab} - x_{ab}y_{ac}}{(x_{ac}y_{ab} - x_{ab}y_{ac})^2 + (x_{ac}z_{ab} - x_{ab}z_{ac})^2 + \beta^2(y_{ac}z_{ab} - y_{ab}z_{ac})^2}$$

$$\times\left\{\frac{x_{bc}x_{ab} + \beta^2(y_{bc}y_{ab} + z_{ab}z_{bc})}{\sqrt{x_{bc}^2 + \beta^2\left(y_{bc}^2 + z_{bc}^2\right)}} - \frac{x_{ac}x_{ab} + \beta^2(y_{ac}y_{ab} + z_{ab}z_{ac})}{\sqrt{x_{ac}^2 + \beta^2\left(y_{ac}^2 + z_{ac}^2\right)}}\right\}$$

$$+\frac{y_{ac}}{y_{ac}^2 + z_{ac}^2}\left[1 - \frac{x_{ac}}{\sqrt{x_{ac}^2 + \beta^2\left(y_{ac}^2 + z_{ac}^2\right)}}\right]$$

$$-\frac{y_{bc}}{y_{bc}^2 + z_{bc}^2}\left[1 - \frac{x_{bc}}{\sqrt{x_{bc}^2 + \beta^2\left(y_{bc}^2 + z_{bc}^2\right)}}\right] \tag{A1}$$

Note that for $M_\infty = 0$, $z = 0$, and $\gamma = 0$, Eq. (A1) reduces to the formula used by Bertin and Smith.[18]

Backwash:

$$u_{ab}\left(\frac{\Gamma}{4\pi}\right)^{-1} =$$

$$\frac{-y_{ac}z_{ab} + y_{ab}z_{ac}}{(x_{ac}y_{ab} - x_{ab}y_{ac})^2 + (x_{ac}z_{ab} - x_{ab}z_{ac})^2 + \beta^2(y_{ac}z_{ab} - y_{ab}z_{ac})^2}$$

$$\times\left\{\frac{x_{bc}x_{ab} + \beta^2(y_{bc}y_{ab} + z_{ab}z_{bc})}{\sqrt{x_{bc}^2 + \beta^2\left(y_{bc}^2 + z_{bc}^2\right)}} - \frac{x_{ac}x_{ab} + \beta^2(y_{ac}y_{ab} + z_{ab}z_{ac})}{\sqrt{x_{ac}^2 + \beta^2\left(y_{ac}^2 + z_{ac}^2\right)}}\right\} \tag{A2}$$

Sidewash:

$$v_{ab}\left(\frac{\Gamma}{4\pi}\right)^{-1} =$$

$$\frac{-x_{ac}z_{ab} + x_{ab}z_{ac}}{(x_{ac}y_{ab} - x_{ab}y_{ac})^2 + (x_{ac}z_{ab} - x_{ab}z_{ac})^2 + \beta^2(y_{ac}z_{ab} - y_{ab}z_{ac})^2}$$

$$\times\left\{\frac{x_{bc}x_{ab} + \beta^2(y_{bc}y_{ab} + z_{ab}z_{bc})}{\sqrt{x_{bc}^2 + \beta^2\left(y_{bc}^2 + z_{bc}^2\right)}} - \frac{x_{ac}x_{ab} + \beta^2(y_{ac}y_{ab} + z_{ab}z_{ac})}{\sqrt{x_{ac}^2 + \beta^2\left(y_{ac}^2 + z_{ac}^2\right)}}\right\}$$

$$+\frac{z_{ac}}{y_{ac}^2 + z_{ac}^2}\left[1 - \frac{x_{ac}}{\sqrt{x_{ac}^2 + \beta^2\left(y_{ac}^2 + z_{ac}^2\right)}}\right]$$

$$-\frac{z_{bc}}{y_{bc}^2 + z_{bc}^2}\left[1 - \frac{x_{bc}}{\sqrt{x_{bc}^2 + \beta^2\left(y_{bc}^2 + z_{bc}^2\right)}}\right] \tag{A3}$$

Note that for $M_\infty = 0$, Eqs. (A1–A3) reduce to the formulas used by Katz and Plotkin.[19]

Acknowledgments

This project is funded by NASA Langley Research Center Grant NAG 1-1852. Part of the work was done under subcontract from Lockheed Martin Aeronautical Systems in Marietta, Georgia. The authors would like to thank Bob Olliffe from Lockheed Martin Aeronautical Systems for the valuable discussions concerning the structural data for the hexagonal wing-box model. The authors want to thank their colleagues Bernard Grossman, Joseph Schetz, William Mason, Phillippe-André, Tétrault, and Andy Ko from the strut-braced wing team for their contributions throughout the project.

References

[1]Pfenninger, W., "Design Considerations of Large Subsonic Long Range Transport Airplanes with Low Drag Boundary Layer Suction," Northrop Aircraft, Inc., Rept. NAI-58-529 (BLC-111), 1958; (available as AD 821759 from Defense Technical Information Center, Alexandria, VA).

[2]Joslin, R. D., "Aircraft Laminar Flow Control," *Annual Review of Fluid Mechanics*, Vol. 30, 1998, pp. 1–29.

[3]Grasmeyer, J. M., Naghshineh-Pour, A. H., Tetrault, P. A., Grossman, B., Haftka, R. T., Kapania, R. K., Mason, W. H., and Schetz, J. A., "Multidisciplinary Design Optimization of a Strut-Braced Wing Aircraft with Tip-Mounted Engines," Multidisciplinary Analysis and Design Center Rept. 98-01-01, Virginia Polytechnic Inst. and State Univ., Blacksburg, VA, Jan. 1998.

[4]Kulfan, R. M., and Vachal, J. D., "Wing Planform Geometry Effects on Large Subsonic Military Transport Airplanes," U.S. Air Force Flight Dynamics Lab., AFFDL-TR-78-16, Wright–Patterson AFB, OH, Feb. 1978.

[5]Park, H. P., "The Effect on Block Fuel Consumption of a Strutted vs. Cantilever Wing for a Short Haul Transport Including Strut Aeroelastic Considerations," AIAA Paper 78-1454, Aug. 1978.

[6]Turriziani, R. V., Lovell, W. A., Martin, G. L., Price, J. E., Swanson, E. E., and Washburn, G. F., "Preliminary Design Characteristics of a Subsonic Business Jet Concept Employing an Aspect Ratio 25 Strut Braced Wing," NASA CR-159361, Oct. 1980.

[7]Grasmeyer, J. M., "Multidisciplinary Design Optimization of a Strut-Braced Wing Aircraft," M.S. Thesis, Virginia Polytechnic Inst. and State Univ., Blacksburg, VA, April 1998.

[8]Gern, F. H., Gundlach, J. F., Ko, A., Naghshineh-Pour, A., Sulaeman, E., Tetrault, P.-A., Grossman, B., Kapania, R. K., Mason, W. H., Schetz, J. A., and Haftka, R. T., "Multidisciplinary Design Optimization of a Transonic Commercial Transport with a Strut-Braced Wing," *1999 World Aviation Congress*, SAE Paper 1999-01-5621, San Francisco, CA, Oct. 1999.

[9]Grossman, B., Strauch, G. J., Eppard, W. M., Gurdal, Z., and Haftka, R. T., "Integrated Aerodynamic/Structural Design of a Sailplane Wing," *Journal of Aircraft*, Vol. 25, No. 9, 1988, pp. 855–860.

[10]Giunta, A. A., Balabanov, V., Haim, D., Grossman, B., Mason, W. H., Watson, L. T., and Haftka, R. T., "Multidisciplinary Optimization of a Supersonic Transport Using Design of Experiments Theory and Response Surface

Modeling," *Aeronautical Journal*, Vol. 101, No. 1008, 1997, pp. 347–356.

[11]Hutchison, M. G., Unger, E. R., Mason, W. H., Grossman, B., and Haftka, R. T., "Variable Complexity Aerodynamic Optimization of a High Speed Civil Transport Wing," *Journal of Aircraft*, Vol. 31, No. 1, 1994, pp. 110–116.

[12]McCullers, L. A., *FLOPS User's Guide, Release 5.81*, NASA Langley Research Center.

[13]Ueda, T., and Dowell, E. H., "A New Solution Method for Lifting Surfaces in Subsonic Flow," *AIAA Journal*, Vol. 20, No. 3, 1982, pp. 348–355.

[14]Lamar, J. E., "A Vortex Lattice Method for the Mean Camber Shapes of Trimmed Non-Coplanar Planforms with Minimum Vortex Drag," NASA TN D-8090, June 1976.

[15]Gimmestad, D., "An Aeroelastic Optimization Procedure for Composite High Aspect Ratio Wings," AIAA Paper 79-0726, April 1979.

[16]Torenbeek, E., "Development and Application of a Comprehensive, Design Sensitive Weight Prediction Method for Wing Structures of Transport Category Aircraft," Delft Univ. of Technology, Rept. LR-693, Delft, The Netherlands Sept. 1992.

[17]"DOT User's Manual," Ver. 4.20, Vanderplaats Research and Development, Inc., Colorado Springs, CO, 1995.

[18]Bertin, J. J., and Smith, L. L., *Aerodynamics for Engineers*, 2nd ed., Prentice–Hall, Englewood Cliffs, NJ, 1989, p. 300, Chap. 7.

[19]Katz, J., and Plotkin, A., *Low-Speed Aerodynamics*, McGraw–Hill, New York, 1991, pp. 379–389, Chap. 12.